



## Identification of tidal mixing fronts from high-resolution along-track altimetry data



Changming Dong<sup>a,b,\*</sup>, Guangjun Xu<sup>a,c</sup>, Guoqi Han<sup>d,\*\*</sup>, Nancy Chen<sup>d</sup>, Yijun He<sup>a</sup>, Dake Chen<sup>c</sup>

<sup>a</sup> Oceanic Modeling and Observation Laboratory, Nanjing University of Information Science and Technology, Nanjing 210044, PR China

<sup>b</sup> Department of Atmospheric and Oceanic Sciences, University of California, Los Angeles, CA 90095-1567, USA

<sup>c</sup> State Key Laboratory of Satellite Ocean Environment Dynamics, Second Institute of Oceanography, SOA, Hangzhou 310012, PR China

<sup>d</sup> Fisheries and Oceans Canada Northwest Atlantic Fisheries Centre, St. John's, NL A1A5J7, Canada

### ARTICLE INFO

#### Keywords:

Tidal mixing fronts  
Satellite altimetry  
20-Hz along-track SSHA  
Hilbert-Huang Transform

### ABSTRACT

Coastal fronts can significantly impact the cross-shelf material exchange and the marine ecosystem. Therefore, it is important to detect their locations and intensities as well as temporal evolutions. In this article, we show that coastal tidal mixing front (TMF) signals can be extracted from both 20-Hz and 1-Hz along-track sea surface height anomalies (SSHA) measured by satellite altimetry. The physical mechanism for the existence of the TMF in the SSHAs data is explained. Then the Hilbert-Huang Transform is applied to selected along-track Jason-2 data over Georges Bank. The extracted fronts have a cross-front sea surface height difference of 13–21 cm over distance of 20–27.5 km. The surface geostrophic current anomalies associated with these fronts are estimated to be 0.38–0.45 m s<sup>-1</sup>, consistent generally with previous studies from in situ observations. The present study clearly demonstrates the potential of satellite altimetry for monitoring TMFs. It is also shown that tidal fronts can be better extracted from the 20-Hz than 1-Hz data.

### 1. Introduction

The cross-shelf exchange of water, nutrient and biomass plays a critical role in the maintenance and evolution of the coastal ecosystem and the protection of the marine environment. A coastal front, which is characterized by the horizontal sharp change in the water density, has significant impacts on the cross-shelf material exchange (Boucher et al., 2013; Lewis et al., 2001; Chen et al., 2003; Dong et al., 2004a, 2014). Therefore, it is important to the coastal environmental study to acquire the location and intensity of a coastal front and their temporal variations.

There are many types of coastal fronts: tidal mixing front (TMF), shelfbreak front, upwelling front and others (Acha et al., 2015). The first two fronts are caused by sharp changes in the bottom topography, among the last one is due to a seaward Ekman transport of the warm sea surface water resulting in upwelling the cold subsurface water near the shore. Though both, a TMF and a shelfbreak front, are related to the bottom topography change, their generation mechanisms are different. For a TMF, on the shoreward side, the water depth is so shallow that the tidal mixing can destroy the stratification and homogenize the whole water column; while on the seaward side, because the water depth is deep, the bottom tidal mixing cannot penetrate the whole water column

and the stratification remains (Boucher et al., 2013). For a shelfbreak front, located over a shelfbreak, it is a conjunction between the coastal water and the open ocean, and the geostrophic constraint due to the sharp topography at the shelfbreak traps the coastal water over the shelf by restraining the open ocean water from entering the shelf. Therefore, the shelfbreak front is more related to a large-scale circulation while the TMF is related to local processes, i.e. tidal mixing. In this paper, we will focus on the TMF.

Unlike upwelling fronts, which are associated with the contrast in the sea surface temperature (SST) identifiable using SST images, a TMF is dominated by the salinity contrast on two sides of the front: fresher water on the shoreward side and saltier water on the seaward side, and most of them are invisible on the SST images. Therefore, we need to appeal to other data to identify them. Though the sea surface salinity (SSS) is measurable by satellite remote sensing, its spatial resolution and accuracy at the present are not good enough for it to be used to identify the coastal TMF. The ocean color data have been applied to detect the TMF (Zhabin and Dubina, 2012). In this study, we propose an approach to identify the TMF from along-track sea surface height anomalies (SSHA) data measured by satellite altimetry and apply it to a well-known TMF over Georges Bank (e.g.: Boucher et al., 2013; Chen et al., 2003; Brink, 2012), which is located on the seaward flank of the

\* Correspondence to: C. Dong, Oceanic Modeling and Observation Laboratory, Nanjing University of Information Science and Technology, Nanjing 210044, PR China.

\*\* Correspondence to: G. Han, Fisheries and Oceans Canada, Northwest Atlantic Fisheries Center, St. John's, NL A1A5J7, Canada.

E-mail addresses: [cmdong@nuist.edu.cn](mailto:cmdong@nuist.edu.cn) (C. Dong), [Guoqi.Han@dfp-mpo.gc.ca](mailto:Guoqi.Han@dfp-mpo.gc.ca) (G. Han).

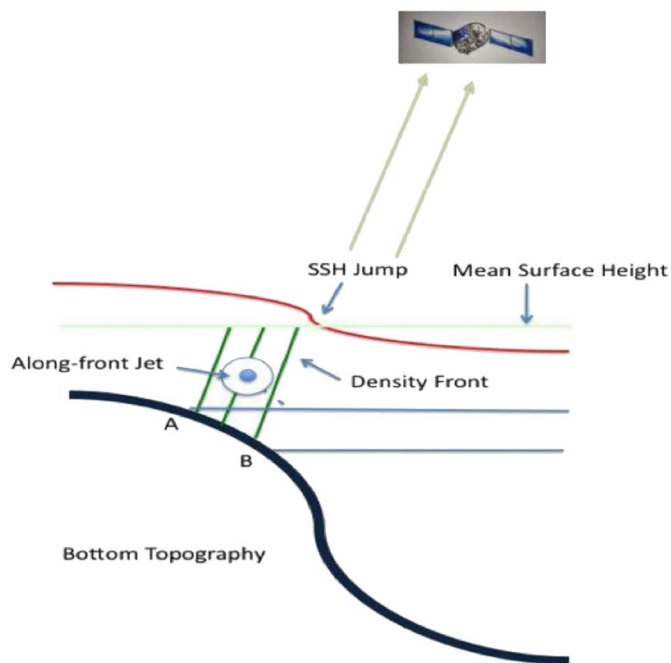


Fig. 1. Illustration of the detection of a coastal front from space. A and B denote two sides of a tidal front. The dot denotes that the along-front jet flows towards readers. The density at A is lower than that at B.

Gulf of Maine in the northwestern Atlantic Ocean.

## 2. Methodology and data

### 2.1. Theory

When a density front is formed, such as a TMF, an along-frontal jet is always accompanied, which in turn introduces a sea surface height anomalies (SSHA) jump across the front with higher sea level on the right side when looking in the direction of the frontal jet in the northern hemisphere (see Fig. 1). The magnitude of the sea level jump across the front depends on many physical factors: the change in the topography, hydrographic conditions of the seawater, and the external forcing, and multiple-scale dynamic processes. The variation of the front is identifiable in the SSHA across the front. Such SSHA jump and its variation should be recorded in the altimeter data when a satellite flies over the front. However due to the complexity in the coastal physical processes, the SSHA jump associated with a TMF across a narrow distance,  $O(10\text{ km})$ , may be contaminated by other processes, like tidal signals, waves, mesoscale and submesoscale eddies pinched off the jet associated with the frontal instabilities (Brink, 2012). Therefore, to extract the TMF signal from the SSHA data, i.e., the SSHA jump, is a challenge. This challenge may in part explain why we could not find any studies on TMF that use conventional 1-Hz along-track SSHA data from satellite altimetry, which have been widely used for studies on other oceanic processes, (e.g. Saraceno et al., 2008; Liu et al., 2012; Roesler et al., 2013; Han et al., 2017; Cipollini et al., 2017). Recently, high-resolution along-track SSHA data from satellite altimetry missions (e.g. Jason-2, Jason-3, SARAL and Sentinel-3A) are available for users to explore new applications (e.g. Han et al., 2012). They are valuable for coastal applications, such as the present application on the coastal tidal fronts. The 20-Hz SSHA data from Jason-2 with an along-track grid of 300 m have much higher small-scale noise than the 1-Hz SSHA data with an along-track grid of about 6 km. To overcome the challenge, we use the 20-Hz along-track SSHA data and employ Hilbert-Huang Transform (HHT) (Huang et al., 1998; Huang and Wu, 2008) (see Methods) in the analysis.

Through a scaling analysis, a non-dimensional momentum equation is derived along the cross-frontal direction ( $x$ -axis, positive seaward) with the assumption that the along-front variation ( $y$ -axis) is negligible (Dong et al., 2004b),

$$P_\eta \frac{\partial \bar{\eta}}{\partial x} = \bar{v} - P_\rho \frac{\partial \bar{\rho}}{\partial x} - P_t \left[ \frac{\partial \overline{u'u'}}{\partial x} + \frac{\partial \overline{u'w'}}{\partial z} \right] \quad (1)$$

where  $\eta$ ,  $\rho$ ,  $v$ , and  $(u', w')$  are the sea surface elevation, sea water density, alongshore current, cross-frontal and vertical tidal currents at the sea surface, respectively. The overbar denotes the average over one tidal period.  $P_\eta$ ,  $P_\rho$  and  $P_t$  are non-dimensional coefficients for the three terms scaled by the Coriolis coefficient: sea surface elevation gradient, density gradient and divergence of the tidal stress, respectively. Eq. (1) shows that the sea surface gradient is balanced by the Coriolis term, density gradient and divergence of the tidal stress. Near the sea surface, the vertical gradient of the second term of the tidal stress ( $\frac{\partial \overline{u'w'}}{\partial z}$ ) can be neglected, therefore integrating Eq. (1) across a tidal front from the onshore side (A) to the offshore side (B) yields (Fig. 1)

$$\bar{\eta}_B - \bar{\eta}_A = \frac{1}{P_\eta} \int_A^B \bar{v} dx - \frac{P_\rho}{P_\eta} (\bar{\rho}_B - \bar{\rho}_A) - \frac{P_t}{P_\eta} (\overline{u_B'^2} - \overline{u_A'^2}) \quad (2)$$

On the right side of Eq. (2), the first term is the cross-frontal integration of the along-frontal jet, which is usually negative (with the higher SSHA on the right when looking towards the jet direction in the northern hemisphere), therefore the first term makes the cross-front sea surface elevation decrease. The second term of Eq. (2) is the surface density difference between the offshore side and the onshore side of the front. In the winter time, a single TMF from the surface to the bottom is observed due to the surface cooling, and the offshore density is larger than onshore density because of the fresher water present near the shore (Dong et al., 2015; see Fig. 3a), which also makes the SSHA decrease across the front from the onshore to offshore; in the summer, on the offshore side, the stratification remains due to the sea surface warming, the offshore density is smaller than onshore density, which increase the SSHA from onshore to offshore (Dong et al., 2015; see Fig. 4a). The third term is the difference in the tidal moment flux across the front, which is positive because the tidal current is smaller on the offshore side than on the onshore side, therefore the third term increases the SSHA from onshore to offshore. In summary, during the wintertime, the first two terms on the right side of Eq. (2) make the SSHA decrease and the third term increases the SSHA from onshore to offshore; during the summertime, the first term makes the SSHA decrease while the second and third terms make the SSHA increase. The non-dimensional parameters in Eq. (1) are  $P_\eta = 0.5$ ,  $P_\rho = 2.5$ , and  $P_t = 5.0$  for Georges Bank (Dong et al., 2004a).

### 2.2. Hilbert-Huang transform

The Hilbert-Huang Transform (HHT) proposed by Huang et al. (1998) and Huang and Wu (2008) is applied in the study. The HHT combines the Empirical Mode Decomposition (EMD) with the Hilbert spectral analysis (HSA). A time series can be decomposed into Intrinsic Mode Functions (IMF) through HHT. Each IMF is an oscillatory mode for the analyzed signal. The approach has been widely used in the scientific and engineering community and their computation scheme is available in the public domain.

By means of obtaining a series of IMFs of any signals, the given signal  $X(t)$  can be reconstructed by

$$x(t) = \sum_{i=1}^n c_i(t) + r(t) \quad (3)$$

where  $c_i(t)$  is the  $i$ th IMF component and  $r(t)$  is the residue. After obtaining all IMF components, the HHT can be applied to each IMF and then the original signal can be expressed by

Download English Version:

<https://daneshyari.com/en/article/8866655>

Download Persian Version:

<https://daneshyari.com/article/8866655>

[Daneshyari.com](https://daneshyari.com)